

Angiogenin promotes angiogenesis via the endonucleolytic decay of miR-141 in colorectal cancer

Chunhua Weng,¹ Haojie Dong,⁴ Rongpan Bai,⁵ Jinghao Sheng,^{2,3} Guangdi Chen,² Kefeng Ding,^{6,7} Weiqiang Lin,¹ Jianghua Chen,¹ and Zhengping Xu^{2,3}

¹Kidney Disease Center, the First Affiliated Hospital, Zhejiang University School of Medicine, 79 Qingchun Road, Hangzhou, Zhejiang 310003, China; ²Cancer Center of the First Affiliated Hospital and Institute of Environmental Medicine, Zhejiang University School of Medicine, Hangzhou, Zhejiang 310058, China; ³Zhejiang Laboratory for Systems and Precision Medicine, Zhejiang University Medical Center, Hangzhou, Zhejiang 311121, China; ⁴Department of Hematological Malignancies Translational Science, Beckman Research Institute, City of Hope Medical Center, Duarte, CA 91010, USA; ⁵Department of General Surgery, Sir Run Run Shaw Hospital, Zhejiang University School of Medicine, Hangzhou, Zhejiang 310020, China; ⁶Department of Colorectal Surgery and Oncology, Key Laboratory of Cancer Prevention and Intervention, Ministry of Education, the Second Affiliated Hospital, Zhejiang University School of Medicine, Hangzhou, Zhejiang 310009, China; ⁷Cancer Center, Zhejiang University, Hangzhou, Zhejiang 310058, China

Mature microRNA (miRNA) decay is a key step in miRNA turnover and gene expression regulation. Angiogenin (ANG), the first human tumor-derived angiogenic protein and also a member of the RNase A superfamily, can promote tumor growth and metastasis by regulating rRNA biogenesis and tRNA production. However, its effect on miRNA has not been explored. In this study, we find that ANG exclusively downregulates mature miR-141 in human umbilical endothelial cells (HUVECs) via its ribonuclease activity and preferably cleaves single-stranded miR-141 at the A⁵/C⁶, U⁷/G⁸, and U¹⁴/A¹⁵ sites via endonucleolytic digestion. By downregulating miR-141, ANG promotes HUVECs proliferation, migration, tube formation, and angiogenesis both *in vitro* and *in vivo*. Conversely, downregulated ANG inhibits ANG-mediated miR-141 decay, thus decreasing the angiogenesis process of HUVECs. We also find an inverse correlation between ANG and miR-141 expression in colorectal cancer (CRC) tissues. Our study indicates that ANG regulates CRC progression by disrupting miR-141 and its regulation on angiogenesis-related target genes, not only revealing a new mechanism of ANG action but also newly identifying miR-141 as a substrate of ANG. This study suggests that targeting ANG nuclease activity might be valuable in treating angiogenesis-related diseases through coordinately regulating the metabolism of rRNA, tRNA, and miRNA.

INTRODUCTION

Angiogenin (ANG), the first human tumor-derived angiogenic protein, was originally isolated from the conditioned medium of HT-29 human colon adenocarcinoma cells based solely on its angiogenic activity.¹ It has now been found to promote tumor growth and metastasis,^{2,3} exhibit microbicidal activity in innate immunity,⁴ enhance neuron outgrowth and survival,^{2,5} differentially regulate stem and progenitor cell quiescence,⁶ and protect intestinal epithelial barrier

integrity⁷ and shape the gut microbe composition⁸ to maintain gut health. However, because of the presence of multiple homologs in model organisms, its physiological and pathological roles and mechanisms of action have not yet been fully elucidated.

ANG is the fifth member of the RNase A superfamily. Although its ribonucleolytic activity is only 10⁻⁵- to 10⁻⁶-fold of what is in RNase A, this activity is essential for ANG to perform its biological functions.² Loss-of-function mutations in the catalytic sites of ANG have been documented in neurodegenerative diseases, such as amyotrophic lateral sclerosis and Parkinson's disease.^{2,9,10} It has long been speculated that certain cellular RNAs can be processed as substrates of ANG, which has been supported by studies on rRNAs and tRNAs.¹¹⁻¹⁴ In the growth state, ANG both enhances rRNA transcription and participates in 47S pre-rRNA processing via endonucleolytic cleavage at the 5' external transcription spacer (A₀ site) to promote cell proliferation.¹¹ However, when under stress, ANG cleaves the anticodon loop of tRNAs to produce tRNA-derived, stress-induced small RNAs (tiRNAs) to maintain cell survival.¹²⁻¹⁴ Therefore, exploring whether ANG can target other RNA subsets as substrates remains of general interest.

Received 1 October 2021; accepted 21 January 2022;
<https://doi.org/10.1016/j.omtn.2022.01.017>.

Correspondence: Dr. Zhengping Xu, Cancer Center of the First Affiliated Hospital and Institute of Environmental Medicine, Zhejiang University School of Medicine, 866 Yuhangtang Road, Hangzhou, Zhejiang 310058, China.
E-mail: zpxu@zju.edu.cn

Correspondence: Dr. Chunhua Weng, Kidney Disease Center, the First Affiliated Hospital, Zhejiang University School of Medicine, 79 Qingchun Road, Hangzhou, Zhejiang 310003, China.
E-mail: chweng@zju.edu.cn

Correspondence: Dr. Jianghua Chen, Kidney Disease Center, the First Affiliated Hospital, Zhejiang University School of Medicine, 79 Qingchun Road, Hangzhou, Zhejiang 310003, China.
E-mail: chenjianghua@zju.edu.cn



Angiogenesis occurs as an orderly cascade of molecular and cellular events that mainly include angiogenic factor secretion; receptor activation and signal transduction; and endothelial cell survival, proliferation, sprouting, migration, tube formation, and vascular stabilization;¹⁵ thus, angiogenesis plays essential roles in several physiological and pathological processes, including embryonic development, wound healing, inflammation, and tumor growth and metastasis.^{16,17} The role of ANG, besides enhancing rRNA biogenesis, in angiogenesis has been well established. ANG can also activate extracellular signal-related kinase 1/2 and protein kinase B/Akt in endothelial cells to produce more ribosomal proteins, thereby promoting cell growth.^{18,19} ANG induces the synthesis of nitric oxide, a well-known regulator involved in vascular physiology, through the PI3K/Akt kinase signaling transduction cascade in endothelial cells.²⁰ In addition, ANG degrades the extracellular matrix and basement membrane to promote endothelial cell invasion and migration into the surrounding tissue.²¹

MicroRNAs (miRNAs) are a class of highly conserved non-coding small RNAs that regulate the expression of target genes post-transcriptionally through translational repression or mRNA degradation.²² Accumulating evidence suggests that miRNAs play critical roles in various bioprocesses, including angiogenesis and tumor progression.^{23,24} To explore the mechanism of action of ANG in angiogenesis and miRNA metabolism, we created a model using human umbilical endothelial cells (HUVECs) and screened for ANG-responsive miRNAs using an miRNA array. We identified miR-141 as one of the most downregulated miRNAs. Coincidentally, our previous results identified miR-141 as a critical angiogenesis-inhibiting miRNA.²⁵ In this study, we first confirmed that ANG downregulated mature miR-141 in HUVECs and then demonstrated that the underlying mechanism for this was endonucleolytic digestion of mature miR-141. We further established the relationship among ANG, miR-141 degradation, and angiogenesis both *in vitro* and *in vivo*. Finally, we provided evidence supporting the roles of ANG-miR-141-targets in tumor angiogenesis and the progression of human colorectal cancer (CRC).

RESULTS

ANG regulates miRNA expression in HUVECs

We adopted HUVECs as the model system to screen differentially expressed miRNAs in responding to recombinant human ANG protein treatment. As the immunofluorescence staining indicated, ANG was internalized and assembled in the cytoplasm and nucleus of the HUVECs (Figure 1A). The miRNA expression profile assay indicated that 25 miRNAs were altered in response to ANG stimulation, including 9 downregulated and 16 upregulated miRNAs with a cut-off fold change of 0.5- or 2-fold compared with the control, respectively (Figure 1B). Of these miRNAs, miR-141 (miR-141-3p) displayed the most striking response to ANG stimulation. We then confirmed the regulation of ANG on miR-141 by quantitative PCR and showed that the miR-141 levels decreased after ANG treatment (Figure 1C) but increased following ANG knockdown in HUVECs (Figure 1D). Consistently, we found that ANG regulated miR-141 levels in the CRC cell line SW480 (Figure S1).

ANG specifically downregulates mature miR-141 in HUVECs

Canonical miRNA biogenesis is a multistep process that involves transcription, processing by Drosha and Dicer, RNA modification, nuclear export, the formation of miRISC (miRNA-induced silencing complex), and RNA decay.²² ANG has been reported to regulate rDNA gene transcription via direct DNA binding, cleave pre-rRNA and tRNA via its ribonucleolytic activity, and modulate various biological processes via interactions with different proteins.² However, its role in miRNA biogenesis remains unknown. To explore whether ANG affects miRNA processing, we measured the amounts of pri-, pre-, and mature miR-141 (miR-141-3p) in HUVECs after treatment with recombinant ANG protein, the depletion of endogenous ANG by siRNAs, or ectopic overexpression of ANG with lentivirus. Quantitative reverse transcription polymerase chain reaction (qRT-PCR) analyses revealed that ANG only regulated mature miR-141 levels but did not change the pri- or pre-miR-141 levels (Figures 1E–1G), suggesting that ANG does not modulate either pri-miR-141 gene transcription or pre-miR-141 processing. miRNA* sequences, which are the fragments from the opposing arm of miRNAs, are typically found at much lower frequencies than the miRNAs.²³ Although miR-141-5p (miR-141*) could not be detected in HUVECs, it could be detected but not regulated by ANG in SW480 cells (Figure S2), suggesting the specificity of ANG's regulation on miR-141.

MiR-141 belongs to the miR-200 family, which includes miR-200a, miR-200b, miR-200c, miR-429, and miR-141. All of these members have very similar sequences, with differences of only several nucleotides. Moreover, miR-200c is located in the same cluster as miR-141, suggesting that they may share the same transcription cassette (Figure S3A). To determine whether ANG affects the levels of other members of the miR-200 family, we also checked the expressions of these four members after ANG was manipulated and found that there were no significant changes, indicating that the regulation of ANG toward miR-141 is specific (Figures S3B and S3C).

The regulation of ANG on miR-141 depends on its ribonuclease activity

Given that ANG is a weak ribonuclease and must enter cells to exert its role,² we examined the contribution of its intracellular enzymatic activity to the downregulation of miR-141. When we treated the cells with RNase inhibitor (RI) or the ANG inhibitor neomycin (Neo)²⁶ to block ANG's activity, ANG's role in regulating miR-141 nearly vanished (Figure 1J). K40 and H114 are two key amino acids in the catalytic center of ANG, and their respective mutants of ANG-K40I and ANG-H114A exhibited null or little RNA hydrolase activity *in vitro* (Figure 1K).²⁷ When we treated HUVECs with either of these two mutants, the downregulation of mature miR-141 was completely abolished (Figure 1L). To determine whether this phenomenon is ANG-specific, we treated the cells with RNase 4 or RNase A, which are two other members of the RNase A family with similar or much stronger enzyme activity compared with ANG (Figure 1K). The results clearly showed that neither RNase was able to downregulate miR-141 in HUVECs (Figure 1L).

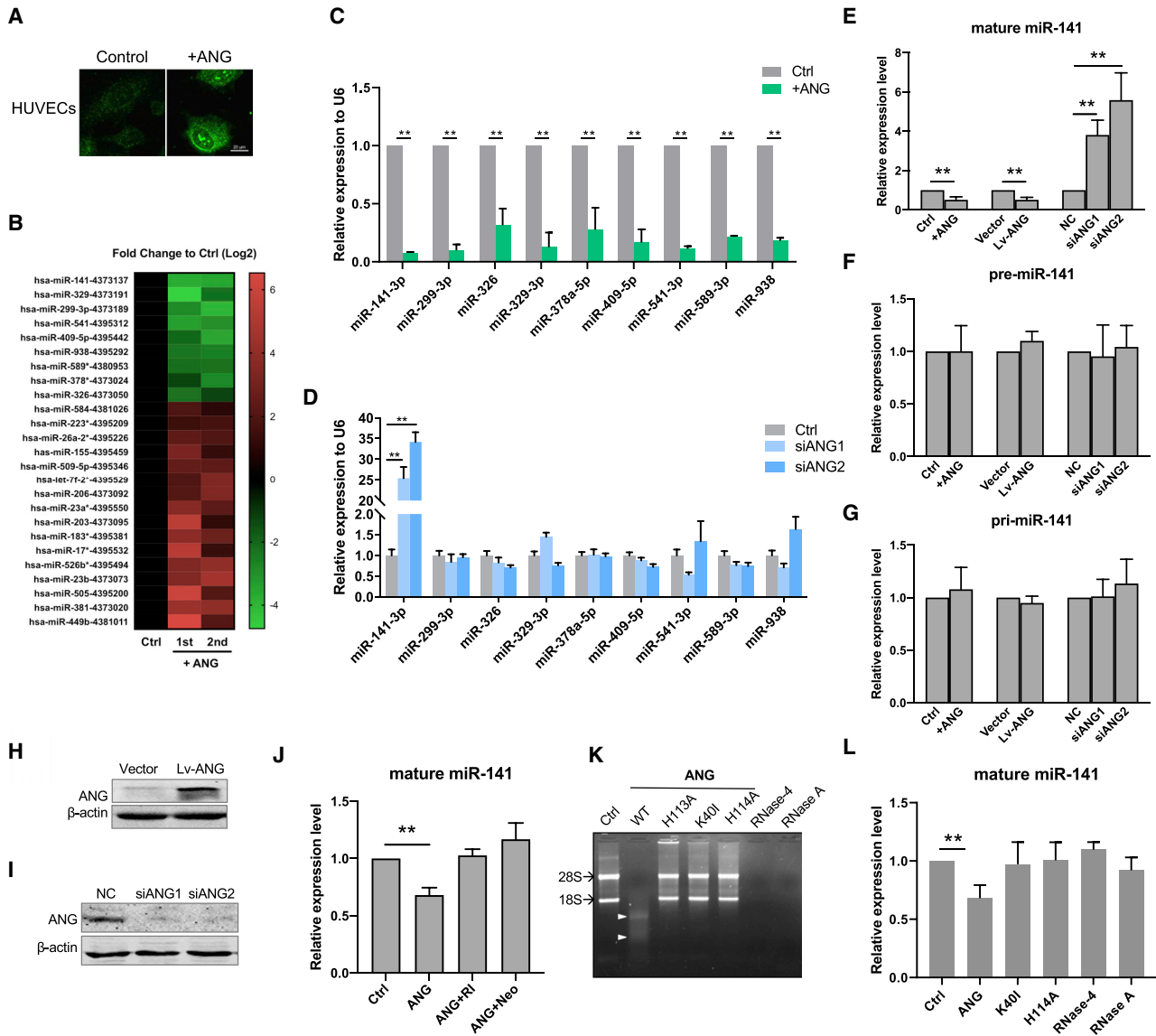


Figure 1. ANG regulates mature miR-141 via its ribonuclease activity in HUVECs

(A) Representative images of immunofluorescence staining of ANG in HUVECs after ANG treatment. Scale bars, 20 μ m. (B) Changed miRNAs in response to ANG treatment screened by TLDA, including 9 downregulated and 16 upregulated miRNAs. (C and D) The downregulated miRNAs were verified by qRT-PCR after ANG treatment or ANG knockdown with siRNA (siANG1 or siANG2) transfection. (E–G) Mature, pre-, and pri-miR-141 levels in HUVECs with ANG treatment, lentivirus-ANG (Lv-ANG) infection, or ANG-targeting siRNA transfection (siANG1 or siANG2). (H and I) Western blot analyses of ANG expression in HUVECs following different treatments as indicated. (J) Mature miR-141 levels in HUVECs after treatment with ANG, ANG + RNase inhibitor (RI), or ANG + neomycin (Neo). (K) RNA electrophoresis of total RNA of HUVECs after treatment with ANG (WT), ANG mutants (K40I or H114A), RNase-4, or RNase A. (L) Mature miR-141 levels in HUVECs after treatment with ANG, ANG mutants (K40I or H114A), RNase-4, or RNase A. The reverse transcription reactions were performed with cell lysate in (B, C, and D), and in (E, J, and L) they were performed with RNA isolated by TRIzol reagent. * $p < 0.05$, ** $p < 0.01$.

We performed an RNA-binding protein immunoprecipitation (RIP) assay with anti-ANG antibodies to explore whether ANG cleaves miR-141 through a direct interaction in cells. The immunoprecipitated RNAs were then purified and analyzed by qRT-PCR and semi-quantitative PCR. The results revealed that only mature miR-141 was enriched by ANG, with no changes in U6, pre-miR-141,

pri-miR-141, or GAPDH mRNA (Figures 2A–2C). To more clearly dissect the localization and interaction between ANG and miR-141, we labeled miR-141 with Cy5 either at the 3' end or the 5' end and used immunofluorescence to visualize ANG. The image revealed obvious co-localization of Cy5-miR-141 with ANG in the cytoplasm in SW480 and HUVEC (Figures 2D and S4).

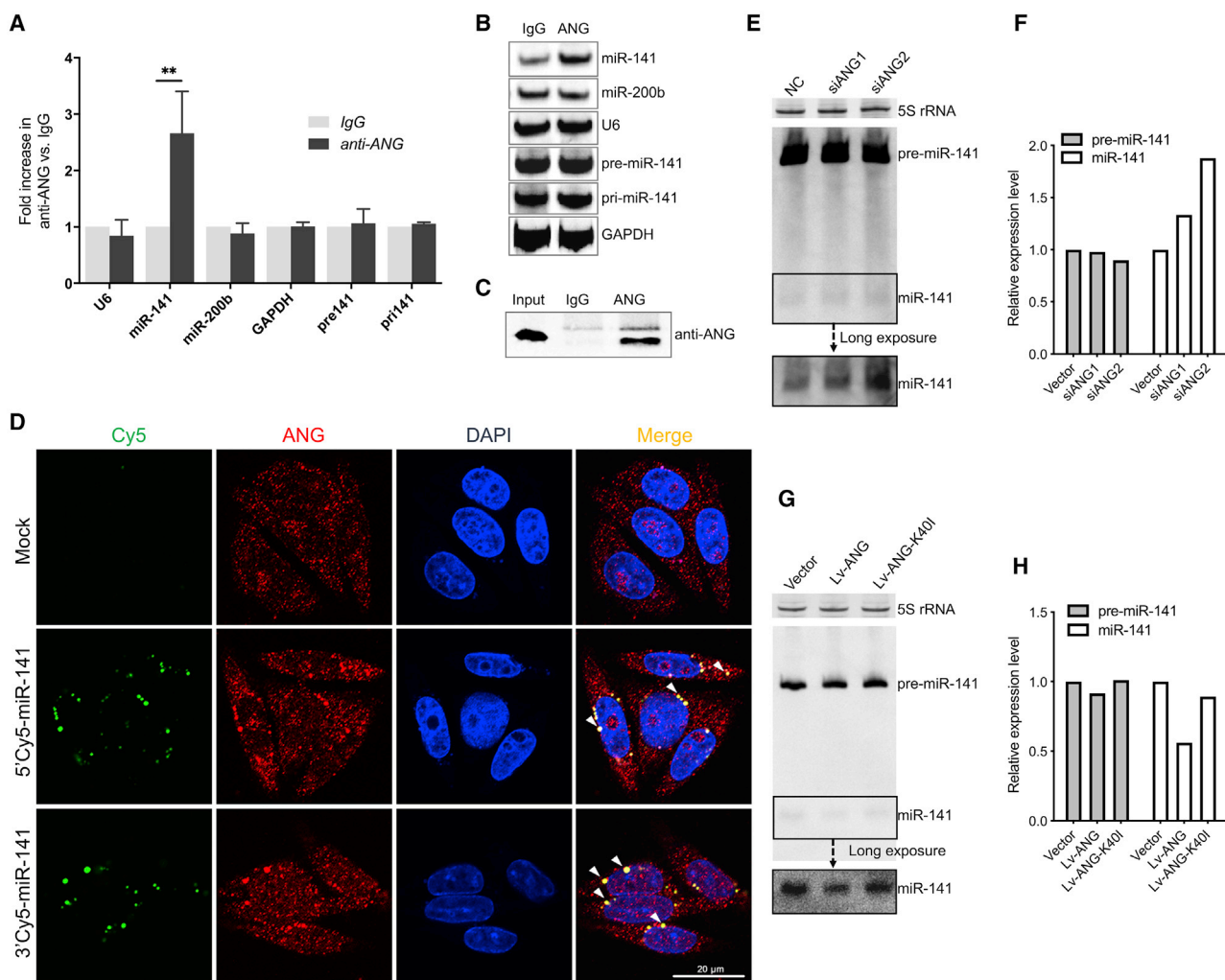


Figure 2. ANG colocalizes with and degrades miR-141 in vivo

(A–C) The interaction between ANG and miR-141 in ANG-overexpressing SW480 cells was detected using the RIP assay. IgG served as a negative control. RNAs in the precipitated complex were determined by qRT-PCR (A) and semi-quantitative PCR (B), including mature, pri-, pre-miR-141, U6 snRNA, and GAPDH mRNA. ANG in the precipitated complex was detected by western blotting (C). (D) Representative images of ANG and miR-141 localization in SW480 cells transfected with 5' end or 3' end Cy5-labeled miR-141. Scale bars, 20 μ m. (E) pre-miR-141 and mature miR-141 were detected by northern blotting in SW480 cells transfected with siRNAs (siANG1 and siANG2) or the negative control. The lower panel shows a longer exposure to visualize the mature miR-141 signal. The 5S rRNA was used as an internal control. The band density was analyzed and is shown in the histogram on the right (F). (G) pre-miR-141 and mature miR-141 were detected by northern blotting in SW480 cells infected with lentivirus-ANG (Lv-ANG), lentivirus-ANG mutant K40I (Lv-ANG-K40I), or lentivirus-vector (Vector). The lower panel shows a longer exposure to display the mature miR-141 signal. 5S rRNA was used as an internal control. The band density was analyzed and is shown in the histogram on the right (H).

To confirm these observations, we further detected pre- and mature miR-141 levels by northern blotting. The results showed that mature miR-141 increased when ANG was knocked down, whereas pre-miR-141 remained at almost the same levels as those of the control group (Figures 2E and 2F). When the cells were infected with the lentivirus to overexpress ANG or ANG-K40I mutant, mature miR-141 decreased only in the ANG-overexpressing cells (Figures 2G and 2H). These results demonstrated that ANG interacts with miR-141 in the cytoplasm and regulates the level of mature miR-141 through its ribonuclease activity.

ANG cleaves single-stranded miR-141 as an endonuclease *in vitro*

To explore the biochemical characteristics and cleavage pattern of ANG in mature miR-141, we developed a cell-free cleavage assay with synthetic miR-141 analogs or its varied forms, including wild-type single-stranded mature miR-141, a single-stranded DNA oligonucleotide with the same sequence of miR-141 (DNA-ss-miR-141), an miR-141 RNA duplex with complete complementary duplex, an miR-141 mimic with complementary duplex with 2-nucleotide 3' overhangs, and a single-stranded miR-141 with different modifications

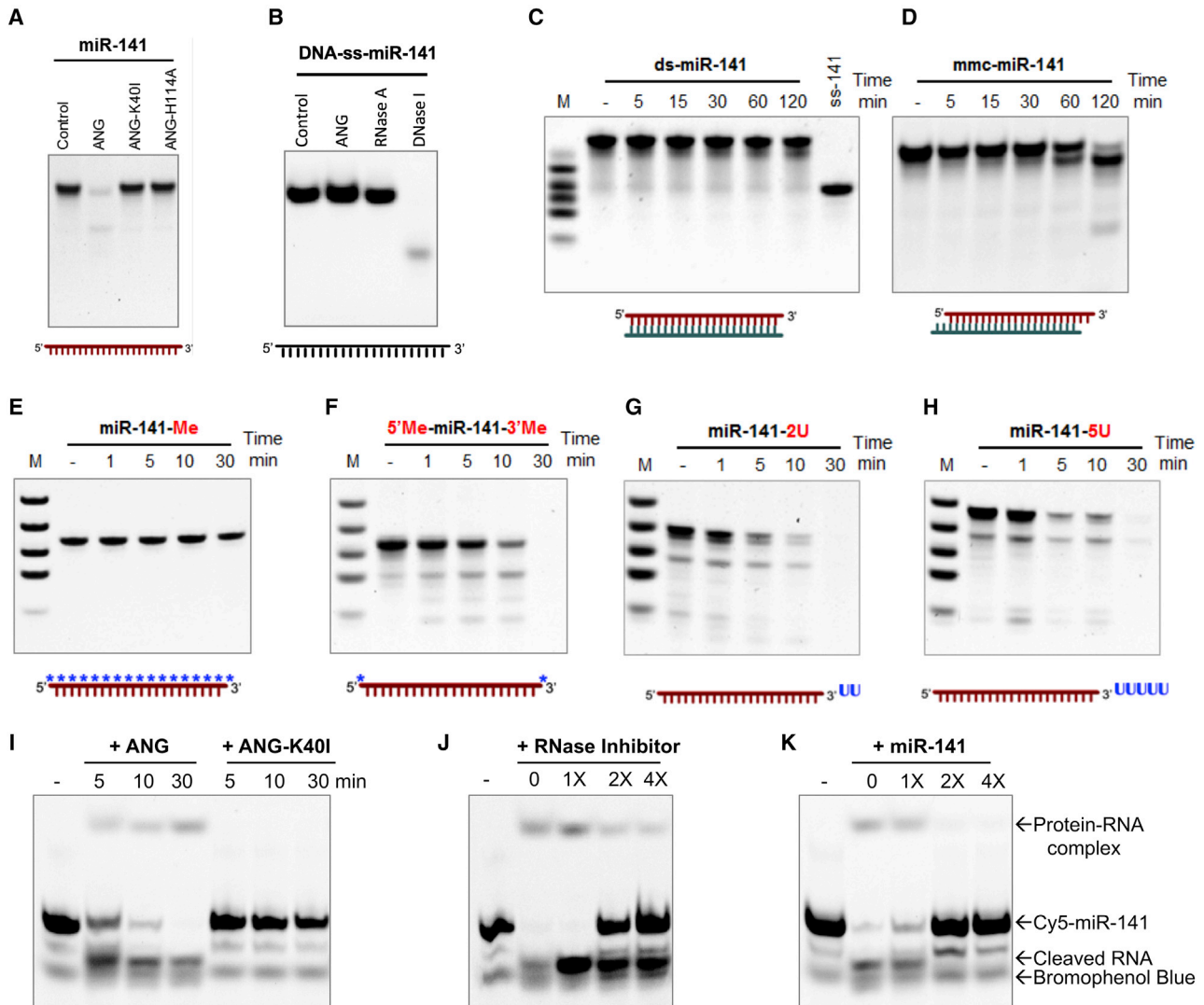


Figure 3. ANG cleaves single-stranded miR-141 as an endonuclease *in vitro*

(A–H) ANG-mediated cleavage of miR-141 was analyzed using cell-free cleavage assays. (A) ANG and its mutants (K40I or H114A) cleave on single-stranded mature miR-141. (B) ANG and its mutants (K40I or H114A) cleave on single-stranded DNA sequence of miR-141 (DNA-ss-miR-141). (C–H) ANG cleaves on miR-141 variants in cell-free cleavage assays at indicated times, including (C) complete complementary duplex of miR-141 (ds-miR-141), (D) miR-141 mimic of complementary duplex with 2-nucleotide (nt) 3' overhangs (mmc-miR-141), (E) single-stranded miR-141 with whole-strand 2'-O-methylation (miR-141-Me), (F) single-stranded miR-141 with 5' end and 3' end 2'-O-methylation (5'-Me-miR-141-3'-Me), (G) single-stranded miR-141 with two additional Us at the 3' end (miR-141-2U), and (H) single-stranded miR-141 with five additional Us at the 3' end (miR-141-5U). (I–K) EMSA was performed to analyze the ANG/miR-141 interaction *in vitro*. Cy5-miR-141 interacted with ANG but not with ANG-K40I (I). RI blocked the binding of ANG to Cy5-miR-141 (J). The binding of ANG to Cy5-miR-141 could be competitively inhibited by unlabeled miR-141 (K). The arrows indicate the protein-RNA complex, free Cy5-miR-141, cleaved miR-141, and bromophenol blue. The color code of the cartoons at the bottom of the gels: red indicates the sequence of miR-141-3p, black indicates DNA sequence of miR-141-3p, green indicates the antisense sequence of miR-141-3p, * indicates 2'-O-methylation.

(methylation or uridylation). The results showed that the synthetic single-stranded miR-141 could be successfully degraded by ANG but not by ANG mutants without ribonuclease activity (Figure 3A). ANG did not digest the DNA sequence of the miR-141 version (Figure 3B) or the miR-141 duplex (Figure 3C). ANG only digested the 3' end overhanging 2-nucleotide of the miR-141 mimic (Figure 3D). Furthermore, the methylated nucleotides were resistant to ANG digestion. When miR-141 was modified with whole-strand nucleotide 2'-O-methyl-

ation, ANG could no longer digest miR-141 (Figure 3E); however, ANG could still cleave the single-stranded miR-141 with 2'-O-methylation at both the 3' and 5' ends (Figure 3F), clearly indicating that ANG cleaves miR-141 as an endonuclease *in vitro* and that nucleotide modified with 2'-O-methylation protects RNA from ANG digestion. Meanwhile, uridylation at the 3' end of single-stranded miR-141 could accelerate ANG digestion on miR-141 to a certain extent (Figures 3G and 3H please compare with Figure 4A).

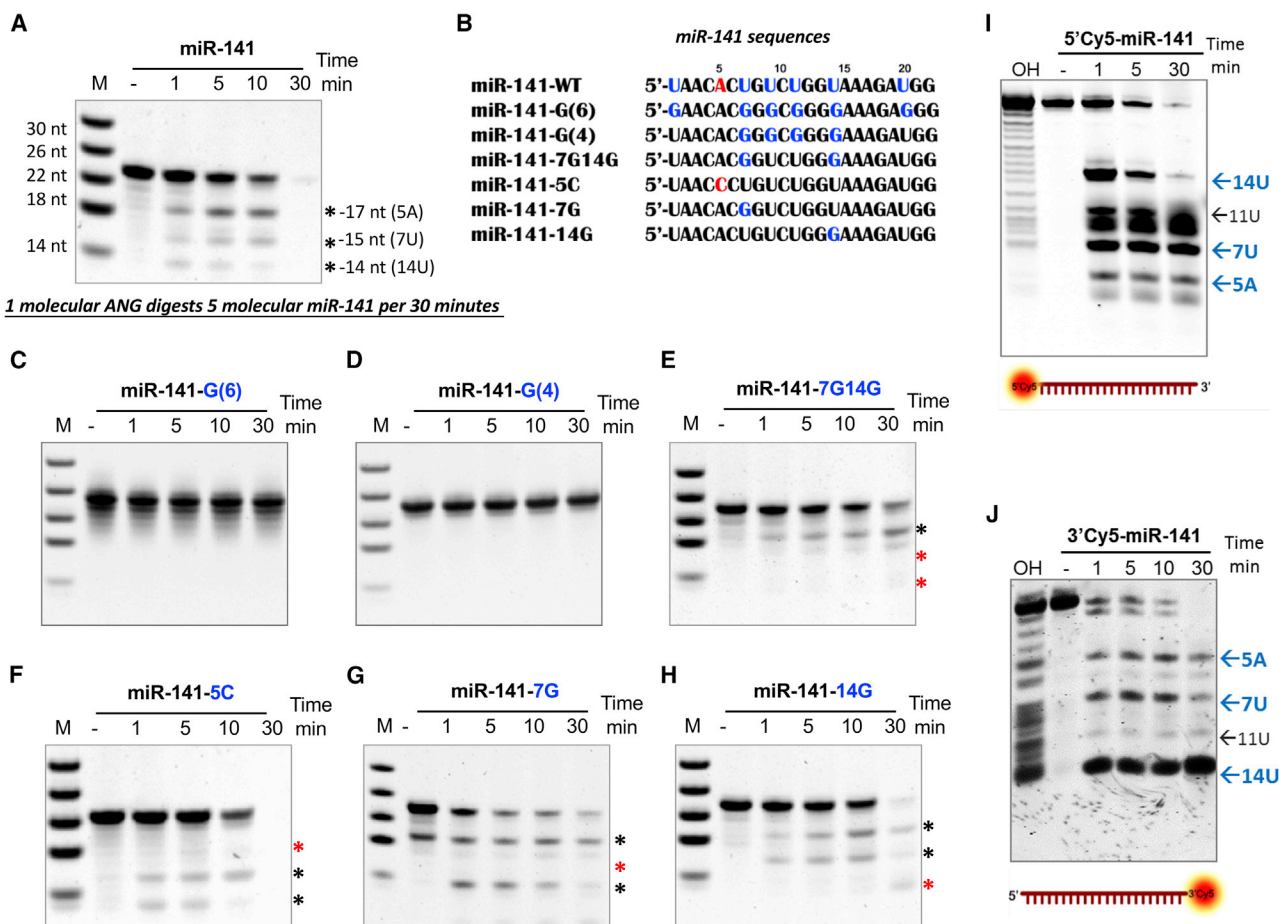


Figure 4. ANG cleaves single-stranded miR-141 at the A⁵/C⁶, U⁷/G⁸, and U¹⁴/A¹⁵ sites

(A) Cleavage pattern of single-stranded mature miR-141 by ANG, *** indicates its main products. The analysis suggested that one molecule of ANG digested five molecules of miR-141 per 30 min. (B) Sequences of wild-type and mutated miR-141 used in this study. (C–H) miR-141 with the indicated mutant sites was incubated with ANG in cell-free cleavage assays for indicated times. The processed samples were separated by urea-denaturing PAGE and stained with SYBR Gold dye. (I and J) 5' or 3' end Cy5-labeled miR-141 was incubated with ANG in cell-free cleavage assays for the indicated times. Lane OH: a reference ladder was generated by alkaline hydrolysis as described in the [Materials and methods](#). The arrows indicate the main cleavage sites according to the urea-denaturing PAGE and fluorescence scanning results.

The electrophoretic mobility shift assay (EMSA) results showed that recombinant ANG interacts with Cy5-miR-141 during cleavage while the mutant ANG-K40I is unable to perform this action ([Figure 4I](#)). The interaction of ANG/Cy5-miR-141 could be blocked by RI ([Figure 4J](#)) or competitively inhibited by unlabeled miR-141 ([Figure 4K](#)). Further analysis revealed that most of the substrate (3.57 pmol/μL) was degraded by ANG (0.71 pmol/μL) in 30 min, indicating that one molecule of ANG is sufficient to cleave five molecules of mature miR-141 in 30 min ([Figure 4A](#)).

ANG cleaves single-stranded miR-141 at the A⁵C⁶, U⁷G⁸, and U¹⁴A¹⁵ sites

We next analyzed the digestion pattern to investigate the cleavage details of ANG on miR-141. Generally, there were three major RNA fragment bands in the SYBR Gold dye-stained gel, corresponding to 17, 15, and 14 nt in length ([Figure 4A](#)). Based on the band length

and the knowledge that ANG preferentially catalyzes RNA after pyrimidine,²⁸ we synthesized a series of mutated miR-141s at certain or all U sites and the 5A site ([Figure 4B](#)). As the results indicate in [Figure 4](#), when more than four Us were replaced by Gs, ANG completely failed to cleave these miR-141 derivatives ([Figures 4C](#) and [4D](#)). When the 7th and 14th U were mutated to G, two major digestion product bands with lengths of 15 and 14 nt were lost ([Figure 4E](#)). When one of the three sites of 5A, 7U, and 14U was replaced, one corresponding cleavage product band was missed ([Figures 4F–4H](#)).

Given that the SYBR Gold dye is not sensitive enough to stain smaller ribonucleotides, we labeled miR-141 with Cy5 at the 5' or 3' ends and then performed the cell-free cleavage assay to further analyze the cleavage site precisely. The data not only confirmed that ANG preferentially digested miR-141 at the A⁵/C⁶, U⁷/G⁸, and U¹⁴/A¹⁵ sites but also indicated other feeble cleavage sites, such as U¹¹/G¹² ([Figures 4I](#) and [4J](#)).

ANG promotes angiogenesis by downregulating miR-141 *in vitro* and *in vivo*

In our previous study, we reported that miR-141 inhibits multiple angiogenesis-related biological processes, indicating that miR-141 plays a powerful and negative regulatory role in angiogenesis.²⁵ To underscore the biological significance of this specific ANG-mediated miR-141 decay, we want to establish the relationship between miR-141-inhibited angiogenesis and ANG-induced angiogenesis. Therefore, we manipulated the levels of ANG and miR-141 in HUVECs and evaluated the coordination of ANG and miR-141 in regulating angiogenesis processes. The results showed that the tube formation inhibition induced by miR-141 could be rescued by adding ANG back into the cell culture medium (Figures 5A–5C) or by overexpressing ANG in HUVECs (Figure S5); this finding suggests that ANG promotes tube formation by downregulating miR-141. Considering that the downregulation of ANG could increase miR-141 levels by attenuating the cleavage effect of ANG on miR-141, we knocked down ANG using siRNAs in miR-141-depleted cells and found that the enhanced tube formation by the miR-141 inhibitor was significantly repressed again (Figures 5D–5F). The reverse effect of ANG and miR-141 was also observed for HUVEC proliferation and migration (Figures 5G and 5H).

To further validate the regulatory axis between ANG and miR-141 in angiogenesis, an *in vivo* Matrigel plug assay was employed. In accordance with the *in vitro* data, fewer vessels in the Matrigel plugs contained agomiR-141, but the vessels were much denser in the Matrigel plugs containing ANG than in the control group (Figures 5I–5K). The combination of agomiR-141 with ANG resulted in a greater median number of vessels than that in the agomiR-141 group but a significantly smaller number than that in the ANG group (Figures 5I–5K), indicating a mutual antagonism between ANG and miR-141 in angiogenic processes *in vivo*. Together, these results indicate that ANG promotes angiogenesis by downregulating miR-141 both *in vitro* and *in vivo*.

ANG, miR-141, target expression, and angiogenesis in colorectal cancer

Angiogenesis is a critical process for solid tumor growth and progression. ANG increases tumor growth while miR-141 has been shown to reduce microvessel density and primary tumor growth.²⁹ To validate our proposed regulatory axis in human samples, we measured the levels of ANG and miR-141 in plasma and tissues from CRC patients and observed a negative correlation between these values (Figures 6A and 6B). We then collected primary colorectal tumors and paired adjacent normal tissues from ten patients with CRC to further investigate the relationships among ANG, miR-141, miRNA-141 targets, and angiogenesis. Our results firstly confirmed the increased microvessel density in tumor tissues (Figures 6C and 6D), and further measurement revealed that ANG mRNA expression was elevated and miR-141 expression was reduced in CRC tissues compared with their adjacent normal tissues (Figures 6E and 6F). Moreover, in the four angiogenesis-related targets of miR-141,²⁵ we found that the protein levels of GATA6 and NRP1 were elevated in tumor tissues (Figures

6G–6K), in accordance with the ANG protein level, which was shown in our previously published article.³ In addition, in the paired CRC cell lines SW480 and SW620, which were established from a primary adenocarcinoma of the colon and a lymph node derived from the same patient, a consistent expression pattern was observed both in the cells and in their cultured medium (Figures 6L–6M).

DISCUSSION

miRNAs play critical roles in nearly all developmental and pathological processes.²² Currently, its biogenesis has been well documented, but the understanding of miRNA turnover is quite limited, particularly in higher organisms. It is generally accepted that miRNA turnover contributes to its homeostasis and represents an important aspect of miRNA regulation. To date, several miRNases (miRNA-degrading nucleases) have been identified, including SDN,³⁰ XRN2,³¹ and RRP6³² in lower organisms, and XRN1,³³ hPNPase^{old-35,34}, Eri1,³⁵ and TSN³⁶ in mammalian cells. Most of these miRNases are exoribonucleases. For example, XRN2 is a 5′-3′ exoribonuclease, and SDN1, RRP6, XRN1, hPNPase^{old-35}, and Eri1 are 3′-5′ exoribonucleases. Until now, TSN was the only endonuclease identified in mature miRNA turnover. Here, we report that ANG could specifically downregulate mature single-stranded miR-141 through endonucleolytic cleavage; both *in vitro* and *in vivo* studies demonstrated that the biological consequence of this downregulation is the induction of angiogenesis. Thus, we not only identified ANG as a miRNA turnover-related endonuclease, but also illustrated a novel mechanism in which ANG and miR-141 regulate angiogenesis.

Although ANG has been studied for more than 30 years, its physiological and/or pathological functions are not yet fully understood.² Very recently, this protein has been reported as a stem/progenitor cell regulator that plays dichotomous roles in reducing the proliferative capacity of primitive hematopoietic stem/progenitor cells (HSPCs) to maintain quiescence while simultaneously facilitating the proliferation of lineage-committed myeloid-restricted progenitor (MycPro) cells.⁶ Mechanistically, this unique function is attributed to cell-type-specific RNA-processing events related to ANG, i.e., tRNA generation in HSPCs and rRNA induction in MycPro cells, both of which are attributed to the endonuclease activity of ANG.⁶ Therefore, the cleavage of ANG on rRNA or tRNA could be a very basic mechanism of action for this multifunctional protein. This study extends the substrates of this protein to include miRNA, which suggests the presence of a novel mode of miRNA turnover in mammalian cells that might be important for rapid changes in miRNA expression profiles during numerous physiological or pathological processes. Although currently we could not identify more different kinds of miRNAs as ANG's substrate, further study would be of interest to explore whether ANG has additional non-coding RNA targets, including long and circular RNAs.

As an endonuclease, the cleavage site of ANG in miR-141 must be identified. According to our results from the cell-free cleavage assay, ANG preferably cuts miR-141 at the A⁵/C⁶, U⁷/G⁸, and U¹⁴/A¹⁵ sites. However, the precise digestion site in the cellular content remains

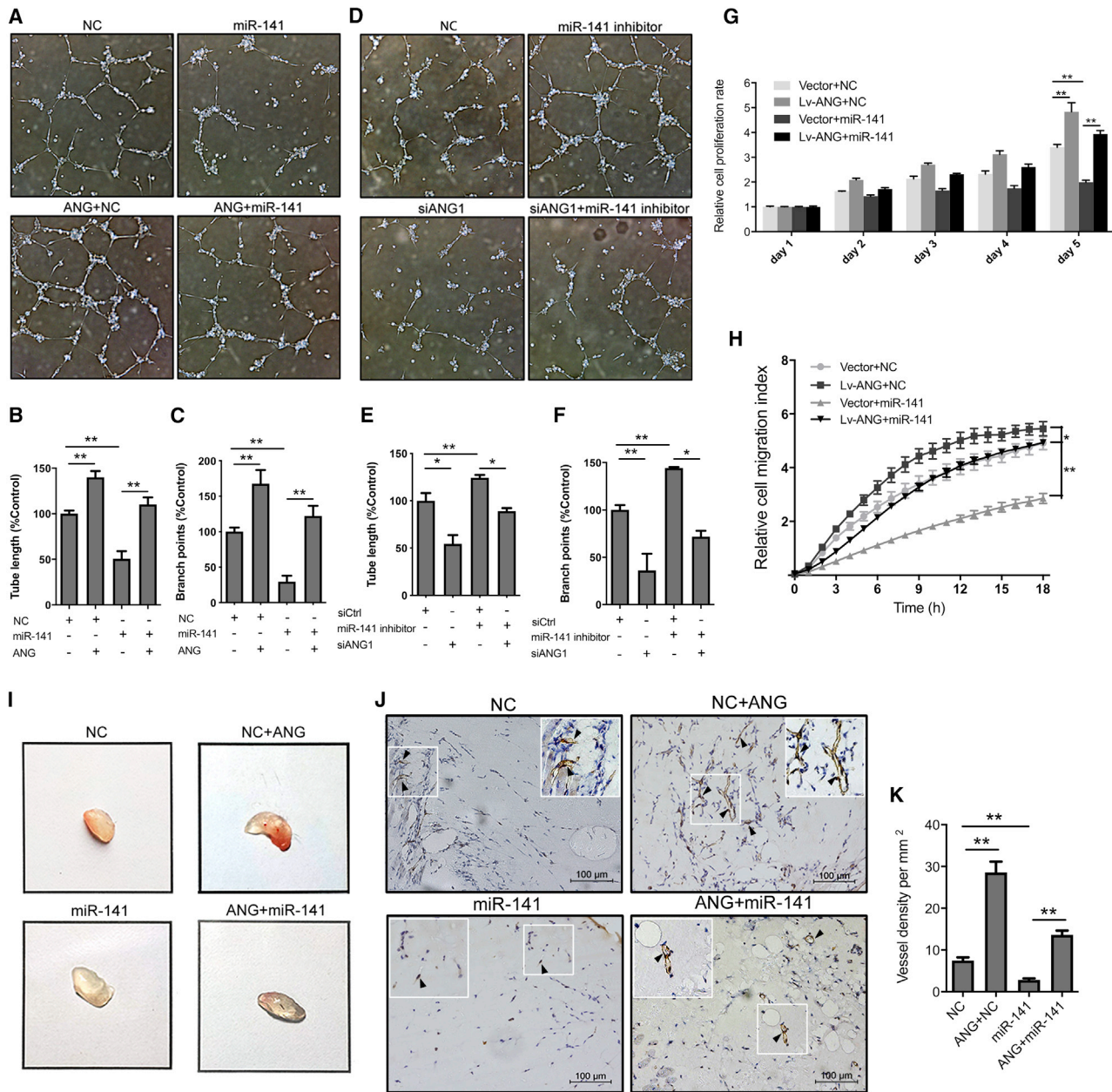


Figure 5. ANG promotes angiogenesis by downregulating miR-141

(A) Representative images of HUVEC tube formation with ANG treatment or miR-141 mimic transfection. (B and C) Statistical analyses of tube lengths and branchpoints. (D) Representative images of tube formation of HUVECs transfected with miR-141 inhibitor and/or siRNA targeting to ANG (siANG1). (E and F) Statistical analyses of tube lengths and branchpoints. (G) HUVEC proliferation using the CCK-8 kit following different treatments as indicated. (H) HUVEC real-time migration using the Roche xCELLigence system following different treatments as indicated. (I–K) HUVEC tube formation *in vivo* following different treatments as indicated. (J) Representative images of CD31 staining in Matrigel plug sections and an enlarged area of the formed vessels. (K) Quantification of vessel density in Matrigel plugs with CD31-positive staining. * $p < 0.05$, ** $p < 0.01$. Scale bars, 100 μm .

unknown. We attempted to assess the digestion products of miR-141 by introducing 5'Cy5- or 3'Cy5-labeled miR-141 into cells, but the cleavage pattern of Cy5-labeled miR-141 differs from that observed in the cell-free system (data not shown). Such a discrepancy could

be due to the interference of Cy5 because the cyanine-dye-labeled oligonucleotide probe could accumulate at the surface of mitochondria;³⁷ alternatively, this modification might change the miR-141 structure in cells as the results showed that miR-141 in a structured

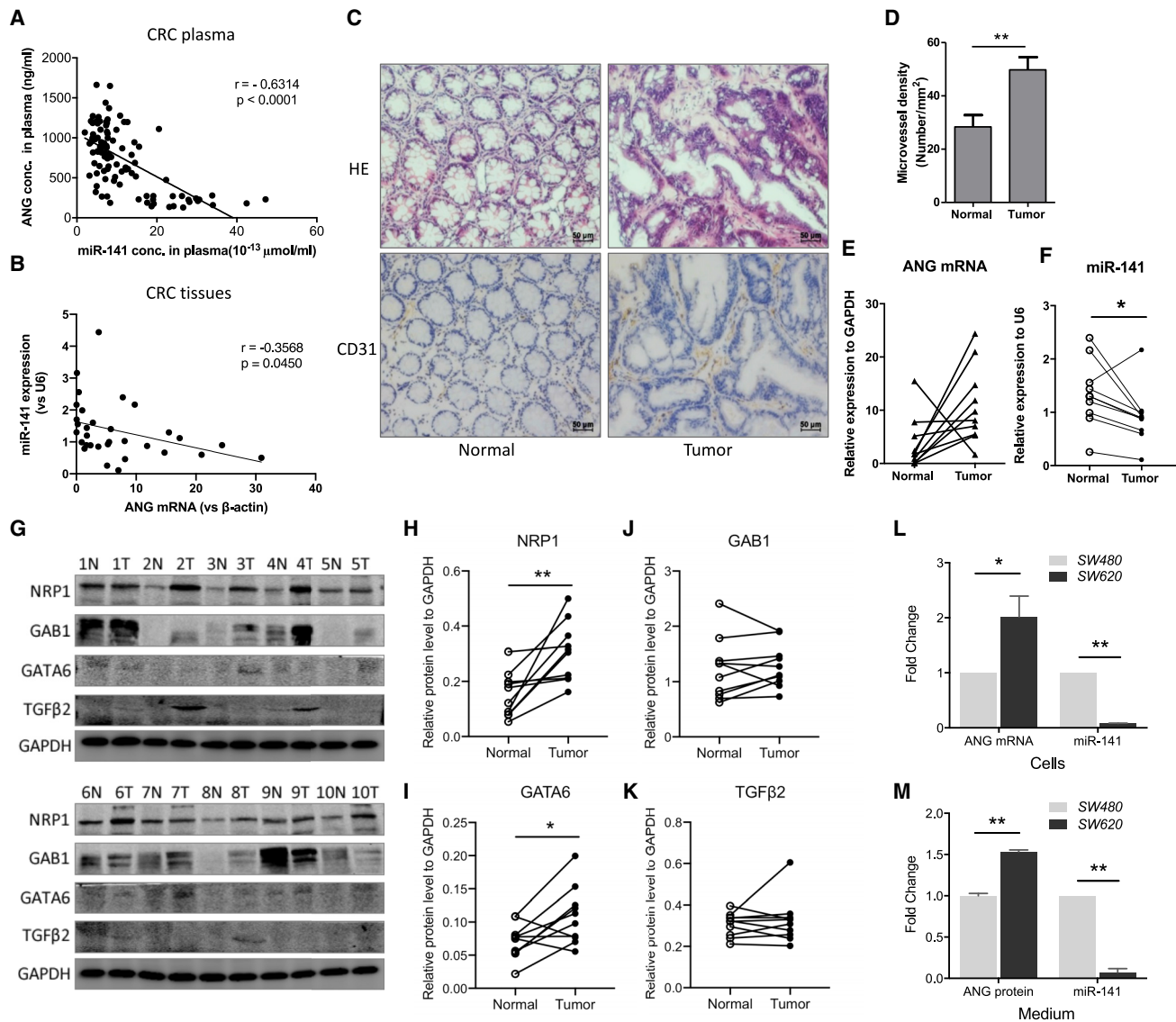


Figure 6. ANG, miR-141, target expressions, and angiogenesis in colorectal cancer

(A) Correlation of the ANG concentration and miR-141 levels in CRC patient plasma. (B) The expression and correlation of ANG mRNA and miR-141 levels in CRC patient and healthy control tissues. (C and D) Microvessels and their density in colorectal cancer and adjacent normal tissues. Microvessels were stained using anti-CD31 antibodies. Scale bars, 50 μm . (E) ANG mRNA expression in CRC and adjacent normal tissues. (F) miR-141 expression in CRC and adjacent normal tissues. (G) Western blotting of miR-141 targets in CRC and adjacent normal tissues. (H – K) Statistical results of the protein gray density in western blot analysis. (L) ANG mRNA and miR-141 expression in SW480 and SW620 cells detected by qRT-PCR. (M) ANG protein and miR-141 levels in SW480 and SW620 culture media. The data represent the mean \pm SD of three independent experiments. * $p < 0.05$, ** $p < 0.01$.

buffer may create a secondary structure that contains a duplex to block ANG digestion (Figure S6). Nevertheless, ANG's recognition and cleavage of its substrate may not be restricted to a specific sequence motif. For example, ANG cleaves 47S pre-rRNA at the A_0 site of "CUC/UUC,"¹¹ but cleaves tRNA at the CA motif of conserved single-stranded 3' CCA termini and the anticodon loop.^{13,38} By contrast, in the cell-free system, ANG degrades 28S and 18S rRNAs into a pattern ranging from 100 to 500 nt in length.³⁹ These findings suggest that auxiliary factors may assist in its cleavage or that a spe-

cific spatial structure may be formed in cells that permit exposure of its digestion site. In addition, a technical limitation is the current lack of an efficient method to effectively capture and analyze RNAs smaller than 18 nt.^{40,41} In fact, we do not know how miRNases, such as exoribonuclease SDN1³⁰ or endonuclease TSN,³⁶ execute their degradation in cells.

Meanwhile, the timing at which ANG cleaves miR-141 remains unknown. Based on our experimental observation, because ANG does

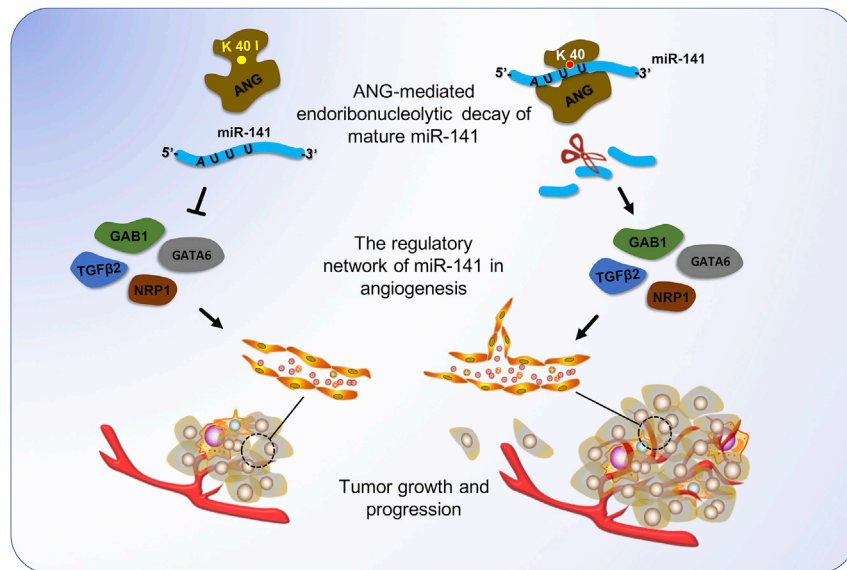


Figure 7. A schematic of ANG-mediated endonucleolytic decay of miR-141 promotes angiogenesis and tumor growth

This schematic shows that ANG cleaves mature miR-141 via direct binding and endonucleolytic digestion depending on its ribonuclease activity. By regulating miR-141 level and its angiogenesis-related targets GAB1, GATA6, TGF- β , and NRP1, ANG promotes the processes of angiogenesis thereby promoting tumor progression.

degrade 28S and 18S rRNAs,³⁹ bind or process mRNA,⁴⁶ and cleave an unknown group of RNAs.⁴⁷ Here, we report that miRNA as a new substrate of ANG, which is a complement for the mechanism of ANG on nucleic acid metabolism. Furthermore, the function of miR-141 was identified to inhibit angiogenesis²⁵ and tumor progression,⁴⁸ demonstrating the rational role of ANG-/miR-141 axis in CRC progression.

not affect pri- and pre-miR-141 in cells, digestion is likely to occur during the single-strand formation stage (Figures 2B and 2C); moreover, ANG does not affect the double-stranded versions (Figures 3C and 3D). It is speculated that ANG cleavage may not occur after miRISC formation because we observed profound effects on miR-141 target expression.²⁵ Therefore, there may be a competing mechanism between ANG and certain RISC components for binding miR-141 at the time of RISC assembly. It is also interesting to observe that ANG only targets miR-141 specifically, although the sequences of miR-200 family members are quite similar. One possible explanation is that these miRNAs may incorporate into different RNA-protein or miRNA-RNA complexes, and the cleavage sites of other members might be shielded from ANG digestion. While, methylation or other types of modification may also affect the interaction between ANG and the members of the miR-200 family, at least methylated nucleic acids were resisted to ANG cleavage as shown in Figure 3E.

Angiogenesis and cancer cell proliferation are required for tumor development, and ANG serves as a critical regulator both in angiogenesis and tumorigenesis. Ribonuclease activity, basement membrane degradation, signaling transduction, and nuclear translocation are considered to be four aspects for the process of ANG-induced angiogenesis.⁴² The secreted ANG undergoes binding to the cell surface actin to promote basement membrane and extracellular matrix degradation, and receptor Plexin-B2⁴³ mediated endocytosis and appropriate sub-cellular localization to activate cell-type-specific signaling and RNA processing. Besides signaling transduction activation, RNA processing is the most critical activity for ANG to participate in the cellular responses involved in angiogenesis and tumor development, including rRNA transcription and tRNA production, as we described in the Introduction. When the activity of ribonuclease or nuclear translocation was deprived, ANG is unable to induce angiogenesis⁹ or tumorigenesis.^{44,45} Meanwhile, ANG can also cleave 47S pre-rRNA¹¹ and

In conclusion, our study provides new insights into the functions and mechanisms of ANG and miR-141 in angiogenesis. We not only identified ANG as an endonuclease involved in miRNA turnover, but we also elucidated a novel angiogenesis regulatory axis of ANG, miR-141, and targets in CRC (Figure 7). Based on these findings, we believe that ANG and miR-141 may have diagnostic and therapeutic values in CRC.

MATERIALS AND METHODS

Cell culture and treatment

The HUVECs were cultured as described previously.⁴⁹ The nuclear translocation of ANG in endothelial cells is required for ANG-induced angiogenesis and is strictly dependent on the cell density. To identify miRNAs that responded to ANG stimulation, the HUVECs were cultured at a density of 5,000 cells/cm² and were starved with FBS-free medium overnight. Subsequently, the cells were incubated with 1 μ g/mL of ANG for 6 h and then harvested for miRNA screening. For miRNA detection assays, 1 μ g/mL of recombinant human ANG, ribonuclease mutated variant ANG-K40I or ANG-H114A, RNase-4 or RNase A, and 200 μ M neomycin or 4 U/mL RI were used to treat HUVECs for 24 h after overnight starvation using FBS-free medium. The recombinant human ANG and its mutants ANG-K40I or ANG-H114A were produced with the bacterial expression system as described previously and confirmed by mass spectrometry analysis.³

miRNA screening

The treated cells were harvested with trypsin and washed with PBS. They were then resuspended in PBS at a density of 2×10^7 /mL. Ten microliters of the cell suspension was lysed in 90 μ L of lysis buffer (15 mM Tris, 10 mM NaCl, 3 mM MgCl₂, 0.3% NP-40) for 10 min on ice, heated at 99°C for 10 min, and then placed on ice again after heating. Six microliters of lysate was used as a reverse transcription

template.⁵⁰ After undergoing reverse transcription with the Human MegaPlex reverse transcription (RT) Primer pools (Applied Biosystems), the TaqMan Low-Density Array Human MicroRNA Cards Set v.2.0 (Applied Biosystems, cat. no. 4400238), which contains 667 mature miRNA probes and four control probes, was used to perform the miRNA expression analysis on the products.

miRNA detection

The treated cells were harvested, and total RNAs were isolated with TRIzol reagent (Life Technologies). The expression levels of individual mature and primary miRNAs were determined by qRT-PCR using the TaqMan miRNA assay kit (Life Technologies). The pre-miRNA level was determined by qRT-PCR using the miScript Precursor Assays kit (QIAGEN). U6 small nuclear RNA was used as an internal control. The data were analyzed using the $\Delta\Delta C_t$ method.

RNA oligoribonucleotides and transfection

When the HUVEC density reached 60%–70% confluence, small RNA transfection was performed with Lipofectamine RNAiMAX (Life Technologies) according to the manufacturer's protocol. The following sequences of siRNAs to ANG were used: siANG1 (sense: 5'-CCAGCACUAUGAUGCCAAATT-3', antisense: 5'-UUUGGCAUCAUAGUGCUGGT-3'); siANG2 (sense: 5'-AAGAAUGGAAA CCCUCACAGA-3'; antisense: 5'-UCUCUGUGAGGGUUUCCAU UC-3'). All small interfering RNA duplexes and miRNA were purchased from GenePharma (Shanghai, China). The negative control small RNAs for the miRNA, siRNA, or miRNA inhibitors were nonhomologous to any human genome sequences and were also provided by GenePharma.

RIP for miRNA

RIP was performed according to the instructions provided with the Magna RIP kit (Millipore). In brief, after being washed with PBS and crosslinked with 1% formaldehyde, ANG-overexpressing SW480 cells were lysed in RIP lysis buffer. The cell lysate supernatant was incubated with protein A/G magnetic beads bound to rabbit anti-ANG polyclonal antibodies (homemade)⁷ or normal IgG. The protein-RNA-bead complexes were collected for RNA detection via qRT-PCR or protein detection via western blotting.

miRNA northern blotting

Northern blotting was performed as described previously⁵¹ with modifications. In brief, 30 μ g total RNA samples resolved on a 17% urea polyacrylamide denaturing gel were transferred to a positively charged nylon membrane (Roche), UV-crosslinked, and probed with DIG-labeled locked nucleic acid (LNA)-modified oligonucleotide probes (Exiqon) overnight at 50°C. The membrane was washed twice at room temperature with low stringency buffer (2 \times SSC, 0.1% SDS) for 5 min, washed twice at 65°C–68°C with high stringency buffer (0.5 \times SSC, 0.1% SDS) for 15 min, and washed once at room temperature with washing buffer for 5 min. After blocking for more than 30 min with blocking solution and incubation with DIG antibodies (Roche), the membrane was washed once with washing buffer for 15 min and balanced in detection buffer (Roche)

for 5 min, followed by incubation with CDP-Star substrate (Roche). The fluorescent signal on the membrane was recorded using the G:BOX Chemi XRQ gel doc system (Syngene).

Cell-free cleavage assay

RNA oligos or duplexes were synthesized by Biomics Biotechnologies and GenePharma. 5'Cy5- or 3'Cy5-labeled RNA oligos were synthesized by Integrated Device Technology. DNA oligos were synthesized by Sangon Biotech. Typically, in a 4- μ L cleavage system, the substrate (2.5 ng/ μ L of Cy5-labeled RNA or 25 ng/ μ L of unlabeled RNA) was incubated with ANG protein (10 ng/ μ L) in DEPC-treated H₂O at 37°C for 30 min or for the indicated time. The reactions were then terminated by the addition of 1 volume of urea loading buffer and put on ice for 5 min; the solution was then subjected to denaturing urea polyacrylamide gel electrophoresis (7 M urea-denaturing 15%–20% polyacrylamide gel with 0.5 \times TBE buffer). Unlabeled oligos in the gels were stained with SYBR Gold dye (Life Technologies), and Cy5-labeled oligos in the gels were scanned using a fluorescence scanner (LI-COR Biosciences). The alkaline hydrolysis ladder was generated by incubating the labeled substrate in alkaline hydrolysis buffer (50 mM NaOH in urea loading buffer) at 80°C for 2–15 min.

EMSA

An EMSA was employed to analyze RNA-protein interactions *in vitro*. Cy5-labeled miR-141 (5 ng/ μ L) was incubated with ANG (10 ng/ μ L) or ANG-K40I (10 ng/ μ L) protein at 37°C for 5–30 min, and Cy5-miR-141 incubated without the protein was used as a control. The specificity of the interaction was tested via blocking studies in the presence of RI or competition studies in the presence of an excess amount of unlabeled miR-141. The following concentrations of RI were used: 0.56 U/ μ L (1 \times), 1.12 U/ μ L (2 \times), and 2.24 U/ μ L (4 \times). Furthermore, 20 ng (1 \times), 40 ng (2 \times), or 80 ng (4 \times) of unlabeled miR-141 were added to compete with the 20 ng of Cy5-miR-141 in the competition reactions. The blocking studies and competition studies were performed during 30 min of incubation at 37°C. The reactions were put on ice for 5 min and then underwent native polyacrylamide gel electrophoresis. RNA-protein complexes and free RNA were visualized using Bio-Rad ChemiDoc MP.

In vitro angiogenesis assay

In vitro angiogenesis assays that assessed the processes of vessel endothelial cell proliferation, migration, and tube formation were performed as described previously.²⁵ The cell proliferation activity of HUVECs was determined using the Cell Counting Kit-8 (Dojindo). Cell migration activity was assessed using the real-time cell migration assays with the xCELLigence RTCA DP instrument (Roche) in CIM-plate 16. The tube formation assay was assessed by the capillary-like structure formation ability of HUVECs on Growth Factor Reduced Matrigel (BD Biosciences).

In vivo angiogenesis assay

The *in vivo* angiogenesis assay was performed using a Matrigel plug assay as described previously.²⁵ ANG alone (1 μ g/mL) or ANG containing 100 μ M agomir-141 (GenePharma) was resuspended in 30 μ L

of PBS and mixed with 500 μ L of Matrigel Basement Membrane Matrix (BD Biosciences) containing 15 units of heparin (Sigma Aldrich). The Matrigel mixture was injected subcutaneously into C57 BL/6 mice (5–7 weeks old) along the abdominal midline. After 6–8 days, the animals were sacrificed to harvest the plug. The angiogenesis ability was quantified by analyzing the immunohistochemical staining of blood vessels with anti-human CD31 antibodies (Abcam). The mice were manipulated and cared for according to the guidelines and protocols approved by the Medical Experimental Animal Care Commission of Zhejiang University (Approval ID ZJU201402-1-01-033).

Tissue specimens

The fresh samples of CRC and the adjacent normal tissues were provided by the tissue bank of the Second Affiliated Hospital of Zhejiang University School of Medicine. Formalin-fixed paraffin-embedded CRC tissues were provided by the tissue bank of the First Affiliated Hospital of Zhejiang University School of Medicine. Plasma samples from CRC patients and healthy individuals were obtained from the Sir Run Run Shaw Hospital, Zhejiang University School of Medicine. All studies were approved by the Ethics Committee of the Zhejiang University School of Medicine (no. 2018-020).

Statistical analysis

The data analyses were performed using GraphPad Prism 8 software. The data are presented as the means \pm SD or percentages of the control \pm SD from at least three independent experiments. The differences in the cell migration curve were analyzed with a two-way ANOVA. The differences in miRNA or mRNA expression among more than two groups and cell proliferation at different time points were analyzed with a one-way ANOVA. The differences between two groups were determined using the two-tailed unpaired Student's *t* test. For the mouse experiments, *n* denotes the number of mice, and $p < 0.05$ was considered statistically significant (* $p < 0.05$, ** $p < 0.01$).

SUPPLEMENTAL INFORMATION

Supplemental information can be found online at <https://doi.org/10.1016/j.omtn.2022.01.017>.

ACKNOWLEDGMENTS

We thank Prof. Liang Xiao for critically reviewing the manuscript and for insightful discussions. This work was supported by grants from the National Natural Science Foundation of China (grant nos. 31300625, 81372303, 31770867, and 31570786); the Zhejiang Provincial Natural Science Foundation of China (grant nos. LY19H050005 and Z206034); the National High-tech Research and Development Program of China (grant no. 2008AA02Z101); and the Fundamental Research Funds for the Central Universities.

AUTHOR CONTRIBUTIONS

Conceptualization, Z.X. and C.W.; methodology, C.W., H.D., R.B., and J.S.; validation, C.W., H.D., and R.B.; formal analysis, C.W., H.D., and R.B.; investigation, C.W., H.D., R.B., J.S., G.C., and W.L.; resources, Z.X., C.W., H.D., R.B., J.S., K.D., and J.C.; data curation, C.W. and H.D.; writing – original draft, C.W. and H.D.; writing – review & editing,

Z.X., C.W., and J.S.; visualization, C.W. and H.D.; supervision, Z.X.; project administration, Z.X. and C.W.; funding acquisition, Z.X. and C.W.

DECLARATION OF INTERESTS

The authors declare no competing of interests.

REFERENCES

- Fett, J.W., Strydom, D.J., Lobb, R.R., Alderman, E.M., Bethune, J.L., Riordan, J.F., and Vallee, B.L. (1985). Isolation and characterization of angiogenin, an angiogenic protein from human carcinoma cells. *Biochemistry* 24, 5480–5486.
- Sheng, J., and Xu, Z. (2016). Three decades of research on angiogenin: a review and perspective. *Acta Biochim. Biophys. Sin (Shanghai)* 48, 399–410.
- Li, S., Shi, X., Chen, M., Xu, N., Sun, D., Bai, R., Chen, H., Ding, K., Sheng, J., and Xu, Z. (2019). Angiogenin promotes colorectal cancer metastasis via tiRNA production. *Int. J. Cancer* 145, 1395–1407.
- Hooper, L.V., Stappenbeck, T.S., Hong, C.V., and Gordon, J.I. (2003). Angiogenins: a new class of microbicidal proteins involved in innate immunity. *Nat. Immunol.* 4, 269–273.
- Li, S., Chen, Y., Sun, D., Bai, R., Gao, X., Yang, Y., Sheng, J., and Xu, Z. (2018). Angiogenin prevents progranulin A9D mutation-induced neuronal-like cell apoptosis through cleaving tRNAs into tiRNAs. *Mol. Neurobiol.* 55, 1338–1351.
- Goncalves, K.A., Silberstein, L., Li, S., Severe, N., Hu, M.G., Yang, H., Scadden, D.T., and Hu, G.F. (2016). Angiogenin promotes hematopoietic regeneration by dichotomously regulating quiescence of stem and progenitor cells. *Cell* 166, 894–906.
- Bai, R., Sun, D., Chen, M., Shi, X., Luo, L., Yao, Z., Liu, Y., Ge, X., Gao, X., Hu, G.F., et al. (2020). Myeloid cells protect intestinal epithelial barrier integrity through the angiogenin/plexin-B2 axis. *EMBO J.* 39, e103325.
- Sun, D., Bai, R., Zhou, W., Yao, Z., Liu, Y., Tang, S., Ge, X., Luo, L., Luo, C., Hu, G.F., et al. (2021). Angiogenin maintains gut microbe homeostasis by balancing alpha-Proteobacteria and Lachnospiraceae. *Gut* 70, 666–676.
- Wu, D., Yu, W., Kishikawa, H., Folkert, R.D., Iafrate, A.J., Shen, Y., Xin, W., Sims, K., and Hu, G.F. (2007). Angiogenin loss-of-function mutations in amyotrophic lateral sclerosis. *Ann. Neurol.* 62, 609–617.
- van Es, M.A., Schelhaas, H.J., van Vught, P.W., Ticozzi, N., Andersen, P.M., Groen, E.J., Schulte, C., Blauw, H.M., Koppers, M., Diekstra, F.P., et al. (2011). Angiogenin variants in Parkinson disease and amyotrophic lateral sclerosis. *Ann. Neurol.* 70, 964–973.
- Monti, D.M., Yu, W., Pizzo, E., Shima, K., Hu, M.G., Di Malta, C., Piccoli, R., D'Alessio, G., and Hu, G.F. (2009). Characterization of the angiogenic activity of zebrafish ribonucleases. *FEBS J.* 276, 4077–4090.
- Yamasaki, S., Ivanov, P., Hu, G.F., and Anderson, P. (2009). Angiogenin cleaves tRNA and promotes stress-induced translational repression. *J. Cell Biol.* 185, 35–42.
- Fu, H., Feng, J., Liu, Q., Sun, F., Tie, Y., Zhu, J., Xing, R., Sun, Z., and Zheng, X. (2009). Stress induces tRNA cleavage by angiogenin in mammalian cells. *FEBS Lett.* 583, 437–442.
- Rashad, S., Niizuma, K., and Tominaga, T. (2020). tRNA cleavage: a new insight. *Neural Regen. Res.* 15, 47–52.
- Adams, R.H., and Alitalo, K. (2007). Molecular regulation of angiogenesis and lymphangiogenesis. *Nat. Rev. Mol. Cell Biol.* 8, 464–478.
- De Palma, M., Bizziato, D., and Petrova, T.V. (2017). Microenvironmental regulation of tumour angiogenesis. *Nat. Rev. Cancer* 17, 457–474.
- Carmeliet, P. (2005). Angiogenesis in life, disease and medicine. *Nature* 438, 932–936.
- Liu, S., Yu, D., Xu, Z.P., Riordan, J.F., and Hu, G.F. (2001). Angiogenin activates Erk1/2 in human umbilical vein endothelial cells. *Biochem. Biophys. Res. Commun.* 287, 305–310.
- Kim, H.M., Kang, D.K., Kim, H.Y., Kang, S.S., and Chang, S.I. (2007). Angiogenin-induced protein kinase B/Akt activation is necessary for angiogenesis but is independent of nuclear translocation of angiogenin in HUVE cells. *Biochem. Biophys. Res. Commun.* 352, 509–513.

20. Trouillon, R., Kang, D.K., Park, H., Chang, S.I., and O'Hare, D. (2010). Angiogenin induces nitric oxide synthesis in endothelial cells through PI-3 and Akt kinases. *Biochemistry* 49, 3282–3288.
21. Hu, G., Riordan, J.F., and Vallee, B.L. (1994). Angiogenin promotes invasiveness of cultured endothelial cells by stimulation of cell-associated proteolytic activities. *Proc. Natl. Acad. Sci. U S A* 91, 12096–12100.
22. Ha, M., and Kim, V.N. (2014). Regulation of microRNA biogenesis. *Nat. Rev. Mol. Cell. Biol.* 15, 509–524.
23. Bartel, D.P. (2004). MicroRNAs: genomics, biogenesis, mechanism, and function. *Cell* 116, 281–297.
24. Annese, T., Tamma, R., De Giorgis, M., and Ribatti, D. (2020). MicroRNAs biogenesis, functions and role in tumor angiogenesis. *Front. Oncol.* 10, 581007.
25. Dong, H., Weng, C., Bai, R., Sheng, J., Gao, X., Li, L., and Xu, Z. (2019). The regulatory network of miR-141 in the inhibition of angiogenesis. *Angiogenesis* 22, 251–262.
26. Hu, G.F. (1998). Neomycin inhibits angiogenin-induced angiogenesis. *Proc. Natl. Acad. Sci. U S A* 95, 9791–9795.
27. Thiyagarajan, N., Ferguson, R., Subramanian, V., and Acharya, K.R. (2012). Structural and molecular insights into the mechanism of action of human angiogenin-ALS variants in neurons. *Nat. Commun.* 3, 1121.
28. Rybak, S.M., and Vallee, B.L. (1988). Base cleavage specificity of angiogenin with *Saccharomyces cerevisiae* and *Escherichia coli* 5S RNAs. *Biochemistry* 27, 2288–2294.
29. Pecot, C.V., Rupaimoole, R., Yang, D., Akbani, R., Ivan, C., Lu, C., Wu, S., Han, H.D., Shah, M.Y., Rodriguez-Aguayo, C., et al. (2013). Tumour angiogenesis regulation by the miR-200 family. *Nat. Commun.* 4, 2427.
30. Ramachandran, V., and Chen, X. (2008). Degradation of microRNAs by a family of exoribonucleases in *Arabidopsis*. *Science* 321, 1490–1492.
31. Chatterjee, S., and Grosshans, H. (2009). Active turnover modulates mature microRNA activity in *Caenorhabditis elegans*. *Nature* 461, 546–549.
32. Ibrahim, F., Rymarquis, L.A., Kim, E.J., Becker, J., Balassa, E., Green, P.J., and Cerutti, H. (2010). Uridylation of mature miRNAs and siRNAs by the MUT68 nucleotidyl-transferase promotes their degradation in *Chlamydomonas*. *Proc. Natl. Acad. Sci. U S A* 107, 3906–3911.
33. Bail, S., Swerdel, M., Liu, H., Jiao, X., Goff, L.A., Hart, R.P., and Kiledjian, M. (2010). Differential regulation of microRNA stability. *RNA* 16, 1032–1039.
34. Das, S.K., Sokhi, U.K., Bhutia, S.K., Azab, B., Su, Z.Z., Sarkar, D., and Fisher, P.B. (2010). Human polynucleotide phosphorylase selectively and preferentially degrades microRNA-221 in human melanoma cells. *Proc. Natl. Acad. Sci. U S A* 107, 11948–11953.
35. Thomas, M.F., Abdul-Wajid, S., Panduro, M., Babiarz, J.E., Rajaram, M., Woodruff, P., Lanier, L.L., Heissmeyer, V., and Ansel, K.M. (2012). Eri1 regulates microRNA homeostasis and mouse lymphocyte development and antiviral function. *Blood* 120, 130–142.
36. Elbarbary, R.A., Miyoshi, K., Myers, J.R., Du, P.C., Ashton, J.M., Tian, B., and Maquat, L.E. (2017). Tudor-SN-mediated endonucleolytic decay of human cell microRNAs promotes G(1)/S phase transition. *Science* 356, 859–862.
37. Rhee, W.J., and Bao, G. (2010). Slow non-specific accumulation of 2'-deoxy and 2'-O-methyl oligonucleotide probes at mitochondria in live cells. *Nucleic Acids Res.* 38, e109.
38. Czech, A., Wende, S., Morl, M., Pan, T., and Ignatova, Z. (2013). Reversible and rapid transfer-RNA deactivation as a mechanism of translational repression in stress. *PLoS Genet.* 9, e1003767.
39. Shapiro, R., Riordan, J.F., and Vallee, B.L. (1986). Characteristic ribonucleolytic activity of human angiogenin. *Biochemistry* 25, 3527–3532.
40. Blumenfeld, A.L., and Jose, A.M. (2016). Reproducible features of small RNAs in *C. elegans* reveal NU RNAs and provide insights into 22G RNAs and 26G RNAs. *RNA* 22, 184–192.
41. Li, Z., Kim, S.W., Lin, Y., Moore, P.S., Chang, Y., and John, B. (2009). Characterization of viral and human RNAs smaller than canonical microRNAs. *J. Virol.* 83, 12751–12758.
42. Gao, X., and Xu, Z. (2008). Mechanisms of action of angiogenin. *Acta Biochim. Biophys. Sin (Shanghai)* 40, 619–624.
43. Yu, W., Goncalves, K.A., Li, S., Kishikawa, H., Sun, G., Yang, H., Vanli, N., Wu, Y., Jiang, Y., Hu, M.G., et al. (2017). Plexin-B2 mediates physiologic and pathologic functions of angiogenin. *Cell* 171, 849–864 e25.
44. Ibaragi, S., Yoshioka, N., Li, S.P., Hu, M.F.G., Hirukawa, S., Sadov, P.M., and Hu, G.F. (2009). Neamine inhibits prostate cancer growth by suppressing angiogenin-mediated rRNA transcription. *Clin. Cancer Res.* 15, 1981–1988.
45. Chavali, G.B., Papageorgiou, A.C., Olson, K.A., Fett, J.W., Hu, G.F., Shapiro, R., and Acharya, K.R. (2003). The crystal structure of human angiogenin in complex with an antitumor neutralizing antibody. *Structure* 11, 875–885.
46. Ivanov, P., Emara, M.M., Villen, J., Gygi, S.P., and Anderson, P. (2011). Angiogenin-induced tRNA fragments inhibit translation initiation. *Mol. Cell* 43, 613–623.
47. Skorupa, A., King, M.A., Aparicio, I.M., Dussmann, H., Coughlan, K., Breen, B., Kieran, D., Concannon, C.G., Marin, P., and Prehn, J.H.M. (2012). Motoneurons secrete angiogenin to induce RNA cleavage in astroglia. *J. Neurosci.* 32, 5024–5038.
48. Gregory, P.A., Bert, A.G., Paterson, E.L., Barry, S.C., Tsykin, A., Farshid, G., Vadas, M.A., Khew-Goodall, Y., and Goodall, G.J. (2008). The miR-200 family and miR-205 regulate epithelial to mesenchymal transition by targeting ZEB1 and SIP1. *Nat. Cell Biol.* 10, 593–601.
49. Weng, C., Dong, H., Chen, G., Zhai, Y., Bai, R., Hu, H., Lu, L., and Xu, Z. (2012). miR-409-3p inhibits HT1080 cell proliferation, vascularization and metastasis by targeting angiogenin. *Cancer Lett.* 323, 171–179.
50. Chen, C., Ridzon, D.A., Broomer, A.J., Zhou, Z., Lee, D.H., Nguyen, J.T., Barbisin, M., Xu, N.L., Mahuvakar, V.R., Andersen, M.R., et al. (2005). Real-time quantification of microRNAs by stem-loop RT-PCR. *Nucleic Acids Res.* 33, e179.
51. Kim, S.W., Li, Z., Moore, P.S., Monaghan, A.P., Chang, Y., Nichols, M., and John, B. (2010). A sensitive non-radioactive northern blot method to detect small RNAs. *Nucleic Acids Res.* 38, e98.